DALTON
FULL PAPER

Very weak electron–electron exchange interactions in paramagnetic dinuclear tris(pyrazolyl)boratomolybdenum centres with extended bridging ligands: estimation of the exchange coupling constant *J* by simulation of second-order EPR spectra †

Peter K. A. Shonfield, Andreas Behrendt, John C. Jeffery, John P. Maher,* Jon A. McCleverty,* Elefteria Psillakis, Michael D. Ward * and Colin Western

School of Chemistry, University of Bristol, Cantock's Close, Bristol, UK BS8 1TS. E-mail: mike.ward@bristol.ac.uk; jon.mccleverty@bristol.ac.uk

Received 11th October 1999, Accepted 29th October 1999

Two series of dinuclear complexes have been prepared in which paramagnetic nitrosylmolybdenum(I) or oxomolybdenum(V) units have been attached to either end of very long bis-pyridyl or bis-phenolate bridging ligands respectively. The first series of complexes is $[\{Mo^{I}(Tp^{Me,Me})(NO)Cl\}_2\{\mu\text{-L}\}]$ (L = 4,4′-bis[2-(4-pyridyl)ethen-1-yl]-biphenyl; 4,4″-bis[2-(4-pyridyl)ethen-1-yl]terphenyl **2**; 4,4′-bis[2-(4-pyridyl)ethen-1-yl]benzophenone **3**; 4,4′-bis[2-(4-pyridyl)ethen-1-yl]benzil **4**; or 6,6′-bis[2-(4-pyridyl)ethen-1-yl]-2,2′-bipyridine **5**). The second series of complexes is $[\{Mo^{V}(Tp^{Me,Me})(O)Cl\}_2(\mu\text{-L})]$ (H_2L = $HOC_6H_4OC(S)OC_6H_4OH$ **6**; $HOC_6H_4OS(O)OC_6H_4OH$ **7**; or $HOC_6H_4OC(O)$-$C_6H_4C(O)OC_6H_4OH$ **8**, with all-*para* substitution for the C_6H_4 units in each case). The very weak spin exchange interactions between the remote paramagnetic centres result in many cases in second-order EPR spectra, because $|J| \approx A$ (where J is the exchange coupling constant, and A the electron–nucleus hyperfine coupling). In these cases the appearance of the EPR spectra is complicated and sensitive to small changes in the magnitude of J, which could be exploited to estimate values for $|J|$ by comparing the measured spectra with computer simulations calculated using a range of values of $|J|$. For the first series of complexes the spin exchange interactions decrease in the order **1** ($|J| \geq 4000$), **2** (1000), **3** (150), **4** (43), **5** ($|J| \leq 10$ MHz) which is readily explicable in terms of the lengths, conformations and substitution patterns of the bridging ligands. For the second series of complexes, **6** and **7** both gave second-order spectra with $|J| = 2000$ MHz, whereas **8**, with a much longer bridging ligand, has $|J| \leq 10$ MHz. Crucially, these spin-exchange interactions are much too weak to be determined by conventional magnetic susceptibility measurements ($|J| \ll 1$ cm^{-1}), and therefore simulation of second-order EPR spectra provides a simple route to providing useful information about the relative magnitudes of very weak spin exchange interactions which is not available by any other route.

Introduction

We have been studying recently the magnetic, electrochemical and spectroscopic properties of polynuclear complexes in which two or more redox-active, paramagnetic tris(pyrazolyl)boratomolybdenum centres are linked by conjugated bridging ligands.[1–5] A significant result of this study has been the demonstration of the role played by the bridging ligand in controlling the sign and magnitude of the coupling constant J for the exchange interaction between the two unpaired metal-centred spins, and we have demonstrated the effects of the length, conformation (planar *vs.* twisted) and topology (substitution pattern) of the aromatic bridging ligands on the value of J.

In all cases we have studied so far the Mo–Mo magnetic exchange interaction has been measured directly by use of a SQUID magnetometer,[2,4,5] which works well when $|J|$ is greater than about 1 cm^{-1}. If $|J|$ is much less than this, *i.e.* if the exchange interaction becomes very weak, then conventional low-temperature susceptibility methods become uninformative. This presents a problem for the study of exchange interactions across very long bridging ligands where the effects of conformation, substitution pattern, *etc.* are potentially just as interesting as they are across shorter ligands where the effects are more easily measured. However in some cases of this sort it is possible to determine the magnitude of the electron–electron exchange coupling constant J even when it is very small, by comparison of the hyperfine components of measured and simulated EPR spectra.

If the two unpaired spins in a diradical are extremely weakly coupled, such that $|J| \ll A$ (where A is the electron–nucleus hyperfine coupling constant), then an EPR spectrum characteristic of isolated, uncoupled paramagnetic centres is observed. We term this behaviour in this paper the 'weak exchange limit'. If however the exchange coupling is stronger such that $|J| \gg A$ then a spectrum is obtained in which both electrons apparently couple to both nuclei and the separation between hyperfine components is halved; this behaviour we call the 'strong exchange limit'.[6] This of course relies on the presence of suitable nuclei with $I > 0$ to which the unpaired spins can couple on both paramagnetic centres. The effect has clearly been demonstrated using molecules containing two nitroxide (amine *N*-oxyl) radical centres having $I = 1$ for the nitrogen nuclei and a sharp, well resolved hyperfine pattern.[7–9] Hydrocarbon diradicals, where the coupling to H atoms provides the necessary hyperfine pattern, can also show this effect.[10] Amongst metal-based polyradicals, spectra showing this 'strong exchange' behaviour between two or more metal centres have been detected for polynuclear vanadium(IV) complexes[11,12] and in our polynuclear molybdenum(I) and molybdenum(V) complexes,[1,13] in both cases the hyperfine pattern of the EPR spectrum being particularly clear and amenable to study in this way.

† *Supplementary data available*: rotatable 3-D crystal structure diagram in CHIME format. See http://www.rsc.org/suppdata/dt/1999/4341/

In the intermediate domain however, when $|J|$ is of a comparable magnitude to A, the appearance of the (second-order) spectrum is much more complicated due to the presence of additional transitions which become vanishingly small at the weak exchange or strong exchange limits.[6] These transitions arise from mixing between the J and A levels when $|J| \approx A$, and are exactly analogous to the additional signals that appear in second-order NMR spectra when the energy of $|J|$ (the coupling constant between two coupled nuclear spins) is comparable in magnitude to that of δ (the chemical shift difference between them). In this domain the appearance of the spectrum is sensitive to small changes in the value of $|J|$ and, if the spectrum can be simulated, this allows an accurate measurement of $|J|$. This has been carried out for some saturated organic diradicals,[7–9] and has also recently been exploited for two series of weakly coupled dinuclear vanadium complexes by Collison, *et al.*[14] and by Elschenbroich *et al.*[15] Vanadium is a particularly suitable metal for studies of this sort because of its isotopic purity and distinctive hyperfine coupling pattern (^{51}V, 100%, $I = 7/2$).

In this paper we report the preparation and EPR spectroscopic study of a series of weakly coupled dinuclear nitrosylmolybdenum(I) or oxomolybdenum(V) complexes, and show how the principles described above could be used to determine reasonable estimates for the value of $|J|$ from EPR spectral simulations. We reported an isolated example of this behaviour a few years ago.[16] The important point for our purposes is that this domain [$|J| \approx A$] covers a range of $|J|$ values (between 10 and 4000 MHz) which are far too weak to be measured by conventional magnetic susceptibility methods. For example, the value of A for the molybdenum complexes we describe here is about 140 MHz, and for the condition $|J| \approx A$ to hold implies values of $|J|$ in the region of 0.005 cm^{-1}.

Results and discussion

EPR spectroscopic properties of the metal complex units

The dinuclear complexes described in this paper are based on the two metal fragments we have used extensively in our recent studies: [Mo^{I}(Tp^{Me,Me})(NO)Cl(py)] [where py is a pyridine donor, and Tp^{Me,Me} is tris(3,5-dimethylpyrazolyl)hydroborate] and [Mo^{V}(Tp^{Me,Me})(O)Cl(OR)] (where OR is a phenolate-type donor).[1] Although in different formal oxidation states, both the nitrosylmolybdenum(I) and oxomolybdenum(V) centres behave very similarly. This is because (i) they both have one unpaired electron in a d_{xy} orbital which is appropriately oriented to interact with the π-symmetry orbitals of the bridging ligands; and (ii) the strong π-electron-withdrawing effect of the nitrosyl group on Mo^{I}, and the strong π-electron-donating effect of the oxo group on Mo^{V}, means that the electron density on each type of metal centre is actually quite similar, and the large difference in oxidation states is more apparent than real.[17]

The two types of mononuclear complex give very similar spectra, which is to be expected given the presence of one unpaired electron in a d_{xy} orbital in each case coupling to a molybdenum nucleus: a central singlet arises from the *ca.* 75% of molybdenum isotopes with $I = 0$, and the surrounding 1:1:1:1:1:1 sextet arises from the remaining *ca.* 25% of molybdenum isotopes with $I = 5/2$. For [Mo^{I}(Tp^{Me,Me})(NO)Cl(py)] complexes, g_{iso} is 1.979(1); for [Mo^{V}(Tp^{Me,Me})(O)Cl(OR)] complexes, g_{iso} is 1.938(1). In both cases the hyperfine coupling constant A_{Mo} is about 50 G‡ and the two spectra look essentially identical apart from their slightly different g values. Likewise, for dinuclear complexes where two of these units are linked by a conjugated bridging ligand, a strong-exchange spectrum is usually seen consisting of a superimposed singlet (from the $I = 0$, $I = 0$ molybdenum isotope combination), 1:1:1:1:1:1 sextet (from the $I = 0$, $I = 5/2$ isotope combination), and 1:2:3:4:5:6:5:4:3:2:1 undecet (from the $I = 5/2$, $I = 5/2$ isotope combination), with a separation of *ca.* 25 G between adjacent hyperfine signals in the multiplets. This occurs even across long bridging ligands, because the condition $|J| \gg A_{Mo}$ is very easily fulfilled: thus the complexes [{Mo^{I}(Tp^{Me,Me})(NO)Cl}$_2${μ-NC$_5$H$_4$(CH=CH)$_5$C$_5$H$_4$N}] (where the bridging ligand has five ethenyl units separating two 4-pyridyl rings, giving an 18-atom pathway between the metals)[19] and [{Mo^{V}(Tp^{Me,Me})(O)Cl}$_2${μ-O(*p*-C$_6$H$_4$)$_4$O}] (where the bridging ligand contains an all-*para* tetraphenylene unit, also giving an 18-atom pathway between the metals)[3] both display strong-exchange spectra. The weak-exchange and strong-exchange limiting forms of these spectra are shown in Fig. 1.[1]

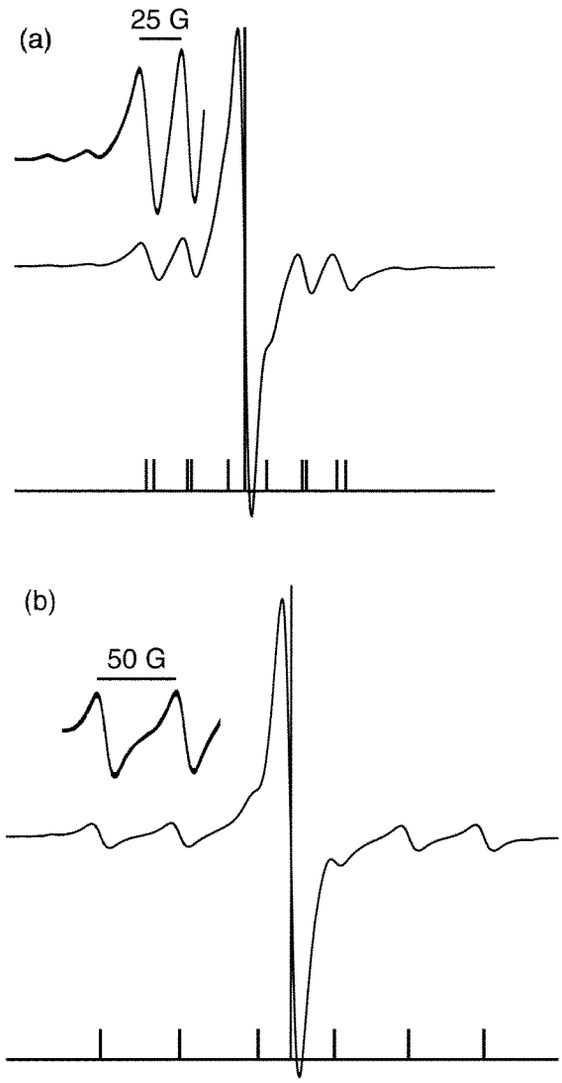

Fig. 1 Simulated EPR spectra for a symmetric dinuclear molybdenum complex with one unpaired electron on each Mo atom; A_{Mo} was taken to be 140 MHz. The values of $|J|$ used are: (a) 4000 MHz (the start of the strong exchange limit), and (b) 0 MHz (the weak exchange limit). The 'stick' spectra at the bottom show the predicted positions of the centres of the components.

Synthesis and characterisation of metal complexes

For this study we required dinuclear complexes with very long bridging ligands that would give weaker exchange couplings than those we had previously observed. To achieve this we prepared ligands that are not only long but also have other structural features that can weaken the exchange interaction across them: *viz. meta* substitution of aromatic rings; saturated fragments; and twisted (as opposed to planar) conformations.

‡ 1 Tesla (T) = 10000 G (G); $\nu = 28.025(g/g_e)B$, with ν in MHz and B in mT (see ref. 18).

Table 1 Characterisation data for the new complexes[a]

Complex	Yield (%)	FAB MS[b,c] *m*/*z*	Elemental analysis[c] (%)		
			C	H	N
1	14	1277 (1278)	52.2 (52.6)	4.8 (5.0)	16.9 (17.5)
2	41	1353 (1353)	54.4 (55.0)	5.4 (5.1)	16.7 (16.6)
3	41	1305 (1305)	52.8 (52.4)	4.2 (4.9)	16.8 (17.2)
4	19	1332 (1332)	52.4 (52.2)	5.1 (4.8)	16.1 (16.8)
5	42	1278 (1280)	49.9 (50.6)	4.8 (4.8)	19.2 (19.7)
6	49	1151 (1150)	45.0 (44.9)	4.3 (4.6)	14.1 (14.6)
7	55	1154 (1154)	43.0 (43.7)	4.8 (4.5)	14.0 (14.6)
8	59	1238 (1238)	48.0 (48.5)	4.4 (4.6)	13.2 (13.6)

[a] In addition complexes **1**–**5** all showed ν_{NO} at 1600–1610 cm^{-1}, and **6**–**8** all showed $\nu_{Mo=O}$ at *ca.* 950 cm^{-1}, in their IR spectra. [b] FAB mass spectra were recorded using 3-nitrobenzyl alcohol as matrix. [c] Calculated values in parentheses. For the mass spectra, the observed and calculated figures quoted are the most intense peak of the isotope envelope in each case.

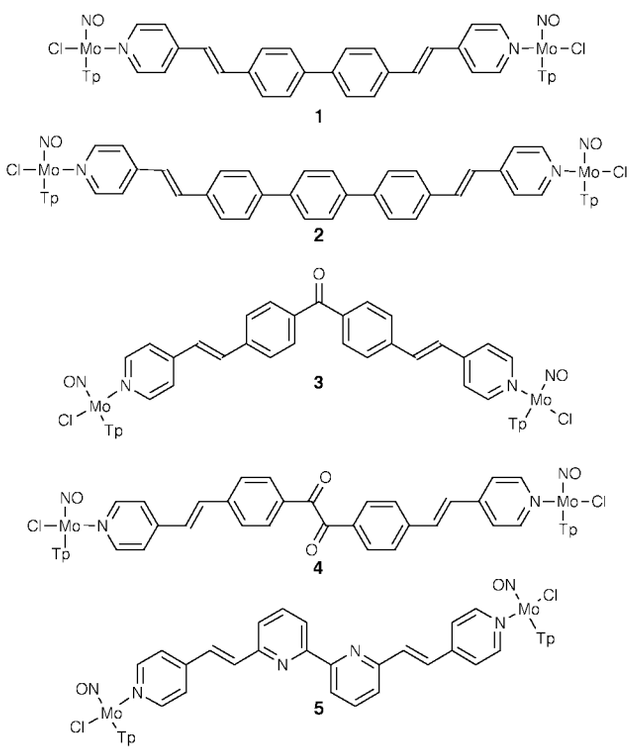

Complexes **1**–**5** all contain two nitrosylmolybdenum(I) units at either end of a bis-pyridyl bridging ligand. Comparison of this series of complexes is intended to illustrate the effects of (i) increasing ligand length, with the central biphenyl unit of **1** extended by one phenylene group in **2**; (ii) increasing distortion away from planarity, with the carbonyl spacers of **3** and **4** resulting in twisted conformations for the bridging ligands; and (iii) substitution pattern, with **5** having two *meta*-substituted aromatic rings at its centre in contrast to **1** which has an all *para* substitution pattern. These complexes were prepared in the usual way by reaction of the bridging ligand with >2 equivalents of $[Mo(Tp^{Me,Me})(NO)Cl_2]$ and Et_3N in toluene at reflux, followed by chromatographic purification; characterisation was on the basis of elemental analyses, IR spectra and FAB mass spectra, whose details are collected in Table 1.

X-Ray quality crystals of complex **3** were obtained and the structure is in Fig. 2. The co-ordination environment about the metal centres is entirely typical of complexes containing $\{Mo(Tp^{Me,Me})(NO)Cl(py)\}$ units.[19,20] The most important point to notice is that the carbonyl group in the centre of the bridging ligand imposes a marked twist between the two adjacent phenyl rings [C(51)–C(56) and C(61)–C(66)] which have an angle of 57° between them; this conformational effect has been seen in many other crystal structures of simple benzophenone derivatives which all have a highly twisted conformation.[21,22] The Mo · · · Mo separation is 22.32 Å. Of course the conformation observed in a crystal structure may not match the solution conformation. Accordingly we performed a molecular modelling study on **3** using the molecular mechanics method implemented on a CAChe workstation,[23] and found that the calculated minimum-energy geometry agreed very closely with the geometry observed in the crystal structure. We note that this minimum-energy geometry will not be the only conformation present in solution given the thermal energy available at room temperature.

Complexes **6**–**8** all contain two oxomolybdenum(V) units at either end of a bis-phenolate bridging ligand. These were prepared by reaction of the mononuclear complex $[Mo(Tp^{Me,Me})(O)Cl(OC_6H_4OH)]$ (complex **A** in Scheme 1), which has a pendant reactive hydroxyl group, with thiophosgene (for **6**), thionyl chloride (for **7**) and terephthaloyl dichloride (for **8**) in toluene/Et_3N at room temperature, followed by chromatographic purification. In this way two pre-formed mononuclear complex units are assembled around a reactive central fragment to give the dinuclear complex, in contrast to **1**–**5** where the complete bridging ligand is prepared first. Analytical and spectroscopic data for these complexes are again collected in Table 1.

Simulations of EPR spectra of dinuclear complexes

Fig. 1 contains simulated EPR spectra for dinuclear molybdenum complexes with one unpaired electron on each metal; they therefore apply equally to both the nitrosylmolybdenum(I) and oxomolybdenum(V) complexes. These show that the appearance of a strong-exchange spectrum (singlet + sextet + undecet, with 25 G separation between components) can be reproduced when $|J| = 4000$ MHz or larger (*i.e.* $|J|/A_{Mo} \geq$ *ca.* 30). Using this value of $|J|$, some second-order splitting is just apparent in the simulation [see the 'stick' spectrum at the bottom of Fig. 1(a)], but once the Lorentzian line broadening has been applied to match the typical observed spectra these closely spaced signals are no longer resolved. The appearance of the simulated spectrum has just reached that of the strong-exchange limiting case at this point, so for any complex exhibiting a spectrum of this type we can only say that $|J| \geq 4000$ MHz. When $|J|$ is reduced to 2000 MHz the additional transitions are clearly resolved and the spectrum is obviously second order (see below). At the other end of the scale, the appearance of a weak-exchange spectrum characteristic of isolated spins is reproduced by simulation with $|J| \leq 10$ MHz (*i.e.* $|J|/A_{Mo} \leq 0.07$); increasing $|J|$ beyond this results in new transitions becoming observable and the clear development of a second-order spectrum.

The simulated spectra in this paper only take into account average hyperfine coupling to the molybdenum nuclei (^{95}Mo and ^{97}Mo, both of which have $I = 5/2$ and similar nuclear

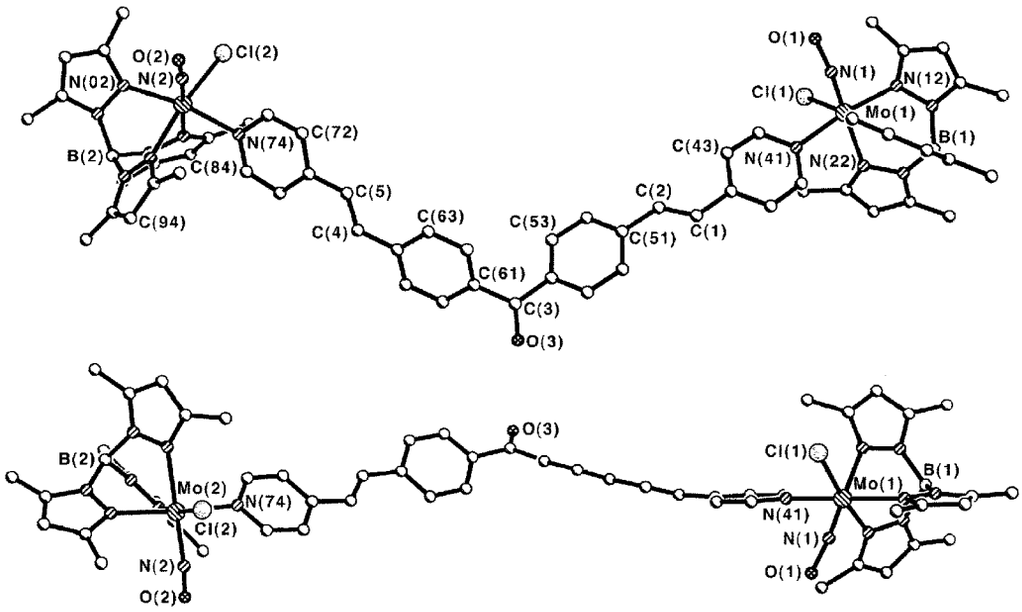

Fig. 2 Two views of the crystal structure of complex **3**.

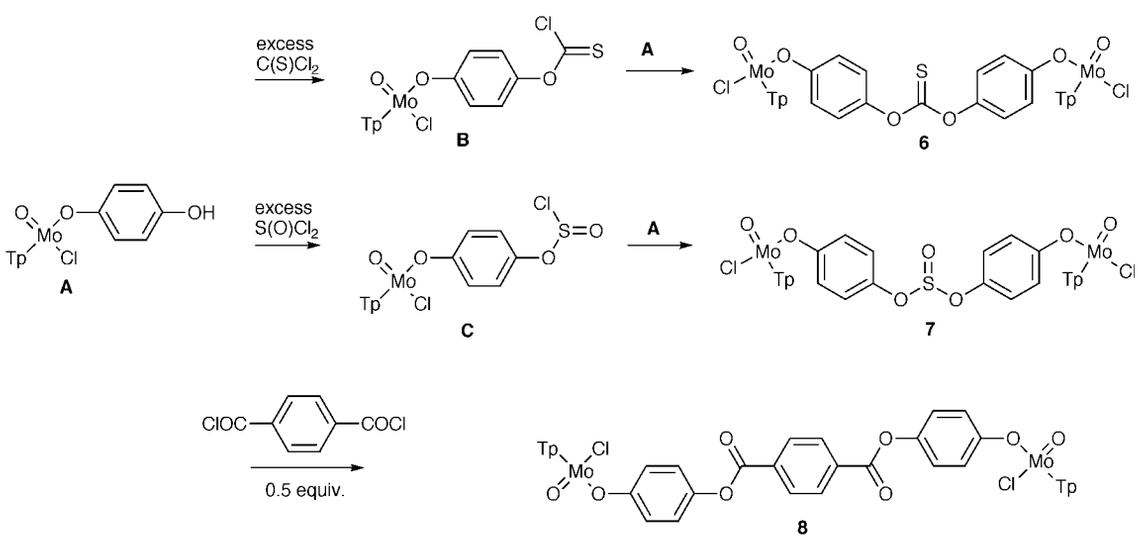

Scheme 1

magnetic moments). ENDOR experiments on complexes of this series have shown that coupling to H, N and B nuclei can also occur,[24] albeit much more weakly, which is also not taken into account in the simulations. In addition the measured spectra exhibit anisotropic line broadening which can be ascribed to (i) tumbling of the entire molecules in solution, and (ii) the internal degrees of freedom of the molecules arising from the conformationally flexible bridging ligands, which will allow one metal unit to rotate with respect to the other about a bond in the bridging ligand. The high-field hyperfine components are accordingly broader and less well resolved than the low-field components (see, for example, Figs. 3 and 5) to an extent which depends on the size, shape and internal flexibility of the complexes.[25] Although it has been possible to simulate line-broadening effects in the spectra of weakly coupled dinuclear vanadium complexes,[14,15] the situation is far more complex for the molybdenum complexes described here because of the presence of several different molybdenum isotopes, which means that each spectrum is a statistical superposition of several contributions. Accordingly we have not attempted to take account of anisotropic line broadening in the simulations. Despite these necessary simplifications, the agreement between real and simulated second-order spectra varies between reasonable and excellent, as we shall demonstrate.

A comment about the fitting of the simulated to the observed spectra is appropriate here. As well as matching 'by eye' the more well resolved low-field part of the measured spectrum to its simulated equivalent, we found that the position of the most extreme low-field hyperfine signal varied smoothly with the value of $|J|$ used for the simulations, so we also used the separation between this signal and the centre line as a guide.

EPR spectroscopic behaviour of the nitrosylmolybdenum(I) complexes

The EPR spectrum of the nitrosylmolybdenum(I) complex **1** is a typical strong-exchange spectrum,[1] so we can only say that $|J| \geq 4000$ MHz for this complex. However for complex **2** (Fig. 3) the spectrum is clearly second order and can be best simulated using $|J| = 1000$ MHz. The spectra of **3** and **4** (Figs. 4 and 5 respectively) are likewise second order and are best simulated using $|J|$ values of 150 and 43 MHz respectively. Finally, the EPR spectrum of **5** is a weak-exchange spectrum characteristic of magnetically isolated spins, *i.e.* $|J| \leq 10$ MHz. Given the extent to which the spectra change as $|J|$ changes, we are confident that our estimated values of $|J|$, derived from comparison of real and simulated spectra, are accurate to within a factor of 2 at worst and in some cases are very much more accurate than

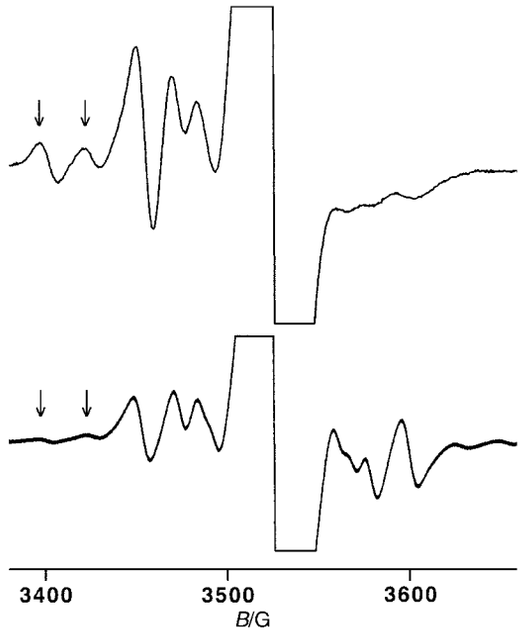

Fig. 3 Observed (top) and simulated (bottom) EPR spectra of complex **2**; the simulation used $|J| = 1000$ MHz.

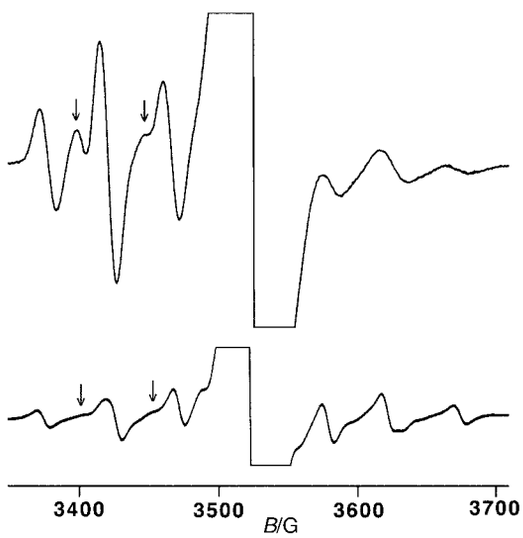

Fig. 4 Observed (top) and simulated (bottom) EPR spectra of complex **3**; the simulation used $|J| = 150$ MHz.

that. We can therefore place these complexes in order according to the strength of the spin exchange interaction: **1** > **2** > **3** > **4** > **5**, with the series spanning the range between the strong-exchange and weak-exchange limits.

We can correlate this ordering of the values of $|J|$ with the properties of the bridging ligands. Thus, the increase in the length of the conjugated bridging ligand from 20 atoms in complex **1** ($|J| \geq 4000$ MHz) to 24 atoms in **2** ($|J| = 1000$ MHz) marks the transition from the lower limit of 'strong exchange' behaviour to the start of 'intermediate' behaviour where second-order spectra result. It is clear that the exchange interaction in **3** ($|J| = 150$ MHz) is weaker than in **2**, despite the bridging ligand being shorter (21-atom pathway across the bridge instead of 24). Given that both bridging ligands are formally completely unsaturated, with all atoms in the bridging pathway being sp^2-hybridised, we suggest that the decrease in $|J|$ for **3** compared to **2** arises from a greater degree of twisting in the bridging ligand arising from the carbonyl groups,[21] as shown by the crystal structure of **3** and the molecular modelling study which showed that this conformation would be retained in solution. The further decrease in the value of $|J|$ on moving

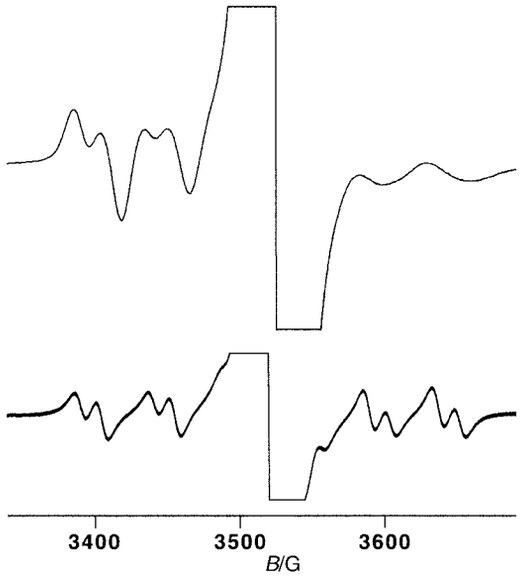

Fig. 5 Observed (top) and simulated (bottom) EPR spectra of complex **4**; the simulation used $|J| = 43$ MHz.

from **3** to **4** ($|J| = 43$ MHz) is consistent with the increased length of the ligand and the conformational distortion induced by the additional carbonyl group.[22] We demonstrated in an earlier paper the importance of the bridging ligand conformation, particularly inter-ring torsions, on the magnitude of magnetic exchange interactions across the ligand as determined by magnetic susceptibility methods.[4]

The effects of topology are shown by comparison of the spectra of complexes **1** and **5**. The shortest pathway linking the metal centres of **5** contains 18 bridging ligand atoms, in contrast to 20 atoms for complex **1**, yet the exchange interaction in **5** is at the weak exchange limit ($|J| \leq 10$ MHz), compared to $|J| \geq 4000$ MHz for **1**. We ascribe this to the effect of the *meta*-substitution pattern of the two central aromatic rings of the bridging ligand in **5**, compared to the all-*para* substitution of **1**. We showed recently that a *meta*,*meta*-substitution pattern in the bridging pathway results in a much weaker spin exchange interactions than does a *para*,*para* pattern, with $[\{Mo(Tp^{Me,Me})(NO)Cl\}_2(\mu\text{-}3,3'\text{-bipy})]$ having $J = -1.5$ cm^{-1}, compared to $[\{Mo(Tp^{Me,Me})(NO)Cl\}_2(\mu\text{-}4,4'\text{-bipy})]$ which has $J = -33$ cm^{-1},[2] and clearly this same effect is operative in complex **5**.

Overall, for this series of complexes the steady decrease in the spin exchange interaction from complex **1** through to **5** is clearly apparent from the EPR spectra and can be rationalised in terms of the lengths, conformations and substitution patterns of the bridging ligands. It is important to remember that this EPR-based method gives us only the *magnitude* of J and not the sign, but nonetheless this is useful information that would not be available by any other means. On the basis of the spin-polarisation model, which we have demonstrated to be generally applicable for more strongly coupled complexes of this type,[1] we expect all of **1**–**5** to be antiferromagnetically coupled; however in the case of very weak couplings, as here, spin polarisation may not be the dominant effect and contributions from other weak coupling mechanisms (such as the dipolar coupling) may become significant.

EPR spectroscopic behaviour of the oxomolybdenum(V) complexes

Complexes **6**–**8** all contain two formally saturated O atoms (other than the phenolate donors, which are common to all of the bridging ligands) in the pathway between the two paramagnetic centres. Thus, even though the bridging ligands are shorter than *e.g.* $[O(p\text{-}C_6H_4)_4O]^{2-}$, which gives a strong-

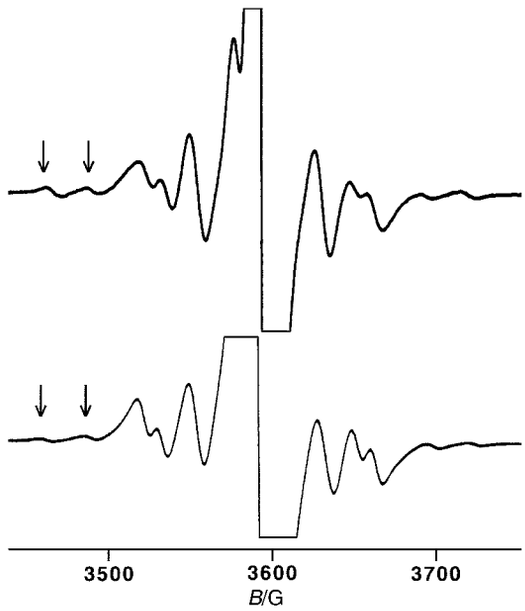

Fig. 6 Observed (top) and simulated (bottom) EPR spectra of complex **6**; the simulation used $|J| = 2000$ MHz.

exchange spectrum across four phenylene units, we might expect the exchange interaction to be weaker, and this turns out to be the case.

The spectrum of complex **6** (Fig. 6) is second order, and could be simulated with $|J| = 2000$ MHz. Unlike the nitrosylmolybdenum(I) spectra described above, those of **6** and **7** in particular do not suffer from anisotropic broadening of the high-field hyperfine components because the bridging ligands are shorter and more flexible, and the agreement between the actual and simulated spectra for **6** is almost perfect. The spectrum of **7**, with an O–S(O)–O bridge in place of the O–C-(S)–O bridge of **6**, results in an essentially identical spectrum also giving $|J| = 2000$ MHz. The only change in the bridging pathway is replacement of a C atom by S, which fortuitously appears to cause no significant change in the magnetic coupling between the oxomolybdenum(V) centres. Extending the bridging ligand further, as in **8** which incorporates an additional phenyl ring, results in a decrease of the exchange interaction to the extent that it can no longer be detected by EPR spectroscopy and a localised, weak-exchange spectrum results, *i.e.* $|J| < 10$ MHz.

Conclusion

It is clear from these studies how determination of the value of $|J|$ from the EPR spectra has provided useful information relating magnetic behaviour to the properties of the bridging ligands. Of course this method can only work when (i) the radical centre concerned has a clear, well resolved hyperfine pattern which lends itself to this sort of analysis (such as the vanadium complexes mentioned earlier),[14,15] and (ii) the exchange interactions are in the domain where $|J| \approx A$ and a second-order spectrum results which is sensitive to small variations in $|J|$ and which can easily be simulated. Both of these features apply to a large number of the Mo–Mo dinuclear complexes studied by our group.[1] Within these constraints the combination of measured and simulated EPR spectra has provided a simple and valuable method for the measurement of weak magnetic exchange interactions.

Experimental

General

The bis-pyridyl bridging ligands used in complexes **1**–**5** were all prepared by a standard[13] Pd-catalysed Heck coupling of 2 equivalents of 4-vinylpyridine with 4,4′-dibromobiphenyl (for **1**), 4,4″-dibromo-*p*-terphenyl (for **2**), 4,4′-dibromobenzophenone (for **3**), 4,4′-dibromobenzil (for **4**) or 6,6′-dibromo-2,2′-bipyridine (for **5**); full details will be published elsewhere.[26] The mononuclear complex precursors $[Mo(Tp^{Me,Me})(NO)Cl_2]$[27] and $[Mo(Tp^{Me,Me})(O)Cl_2]$[28] were prepared according to the literature methods. Other reagents were purchased from the usual commercial sources (Aldrich, Lancaster) and used as received.

EPR spectra of solutions of the complexes in degassed CH_2Cl_2 at room temperature were recorded with a Bruker ESP-300E instrument (X-band). Typical parameters were as follows: modulation frequency, 100 kHz; modulation amplitude, 1 G; microwave power, 20 mW; microwave frequency, 9.5–9.8 GHz.

EPR spectral simulations

To calculate the energy levels, the effective Hamiltonian of Reitz and Weissman was used,[6] eqn. (1). The other possible

$$\hat{H} = g_e\mu_B B_z(\hat{S}_{1z} + \hat{S}_{2z}) - g_{iso}\mu_N B_z(\hat{I}_{1z} + \hat{I}_{2z}) + J\hat{\boldsymbol{S}}_1\cdot\hat{\boldsymbol{S}}_2 + A\hat{\boldsymbol{S}}_1\cdot\hat{\boldsymbol{I}}_1 + A\hat{\boldsymbol{S}}_2\cdot\hat{\boldsymbol{I}}_2 \quad (1)$$

couplings ($\hat{\boldsymbol{S}}_1\cdot\hat{\boldsymbol{I}}_2$, $\hat{\boldsymbol{S}}_2\cdot\hat{\boldsymbol{I}}_1$ and $\hat{\boldsymbol{I}}_1\cdot\hat{\boldsymbol{I}}_2$) can be ignored. The Hamiltonian matrix was set up for each value of total $M = m_{S1} + m_{S2} + m_{I1} + m_{I2}$ including all possible combinations and diagonalised. Transition intensities were then calculated by taking the matrix elements of the Zeeman Hamiltonian between basis states with adjacent values of M and transforming with the eigenvalues taken from the diagonalisation. The resulting spectrum was then convoluted with a sine function corresponding to the modulation amplitude, and a Lorentzian function adjusted to give the observed linewidth. The J values were adjusted to give the best agreement between observed and calculated spectra.

Preparations

Dinuclear complexes 1–5. A mixture of the appropriate ligand (1.0 mmol), $[Mo(Tp^{Me,Me})(NO)Cl_2]$ (1.25 g, 2.5 mmol) and dry Et_3N (2 cm^3) in dry toluene (80 cm^3) was stirred and heated to reflux under N_2 for 24 h. After removal of the solvent *in vacuo* the residue was purified by column chromatography on silica gel, eluting with the following solvent mixtures: for **1**–**4**, CH_2Cl_2–thf (98 : 2); for **5**, CH_2Cl_2–thf (96 : 4).

Mononuclear complex $[Mo(Tp^{Me,Me})(O)Cl(OC_6H_4OH)]$ (Scheme 1, compound A). A mixture of $[Mo(Tp^{Me,Me})(O)Cl_2]$ (1.0 g, 0.15 mmol), hydroquinone (0.50 g, 0.45 mmol, a large excess) and NaH (0.10 g, 0.42 mmol) in dry toluene (50 cm^3) was stirred and heated to 80 °C under N_2 for 48 h. The solution was then filtered to remove excess of hydroquinone and the solvents removed *in vacuo*. Purification by chromatography on silica gel eluting with CH_2Cl_2–thf (99 : 1) afforded the product as a slow-running dark blue band, which was isolated by combining and concentrating the relevant fractions and then adding excess of hexane to precipitate the product. Yield: 35%. Found: C, 45.9; H, 5.0; N, 15.1. Required for $C_{21}H_{27}BClMoN_6O_3$: C, 45.6; H, 4.9; N, 15.2%. FAB MS: *m*/*z* 555 (100%, M^+).

Dinuclear complex 6. To a stirred mixture of $[Mo(Tp^{Me,Me})(O)Cl(OC_6H_4OH)]$ (0.15 g, 0.27 mmol) and dry Et_3N (0.5 cm^3) in dry toluene (30 cm^3) under N_2 was added thiophosgene (0.5 cm^3, a large excess) by syringe. After stirring for 10 min at room temperature the solvent and excess of thiophosgene were removed by evaporation. The resulting solid (intermediate **B**, see Scheme 1) was redissolved in dry

toluene (30 cm^3) and dry Et_3N (0.5 cm^3); another portion of [Mo($Tp^{Me,Me}$)(O)Cl(OC_6H_4OH)] (0.15 g, 0.27 mmol) was added and the solution stirred for 10 min at room temperature. After evaporation of the solvent the crude product was purified by column chromatography (silica, CH_2Cl_2) to yield pure complex **6** as a dark red solid.

Dinuclear complex 7. This was prepared and purified in exactly the same way as complex **6**, but using thionyl chloride in place of thiophosgene during the synthesis to give intermediate **C** (see Scheme 1).

Dinuclear complex 8. To a mixture of [Mo($Tp^{Me,Me}$)(O)Cl(OC_6H_4OH)] (0.30 g, 0.54 mmol) and terephthaloyl dichloride (0.050 g, 0.25 mmol) in dry toluene (30 cm^3) under N_2 was added Et_3N (0.5 cm^3) at room temperature. After stirring the mixture for 10 min, the solvent was evaporated and the crude solid purified by column chromatography (silica, CH_2Cl_2) to yield pure complex **8** as a dark red solid.

Yield, spectroscopic and analytical data for complex **1**–**8** are collected in Table 1.

X-Ray crystallography

Crystal data for complex 3·3Et_2O. $C_{69}H_{94}B_2Cl_2Mo_2N_{16}O_6$, $M = 1528.0$, triclinic, space group $P\bar{1}$, $a = 15.366(3)$, $b = 16.789(3)$, $c = 18.212(4)$ Å, $\alpha = 107.15(3)$, $\beta = 110.24(3)$, $\gamma = 104.79(3)°$, $V = 3863.0(1.3)$ $Å^3$, $T = 173$ K, $Z = 2$, μ(Mo-Kα) = 0.452 mm^{-1}. 28101 Reflections were measured with $2\theta_{max} = 50°$, which after merging afforded 12793 unique data ($R_{int} = 0.0536$). All data were used in subsequent calculations. Final $wR2$ (all data) = 0.250; $R1$ [based on selected data with $I > 2\sigma(I)$] = 0.092. The instrument used was a Siemens SMART-CCD diffractometer. Software used: SHELXS 95 for structure solution;[29] SHELXL 95 for structure refinement;[29] SADABS for the absorption correction.[30]

Crystals of complex **3**·3Et_2O were fragile and lost solvent easily; despite rapid mounting of the crystal at 173 K some decomposition occurred. In addition there is extensive disorder of the lattice solvent molecules, and also disorder between the nitrosyl and chloride groups on each metal. One molecule of Et_2O was well behaved, but there was also a large collection of electron-density peaks which were assigned as carbon atoms with fractional site occupancies of 0.5 or 1.0 and refined with isotropic thermal parameters; the total of these corresponded to approximately 2 more ether molecules. The formulation of the crystal as containing three ether molecules per complex unit is therefore approximate. The combination of solvent loss and substantial disorder resulted in weak data, which accounts for the modest quality of the refinement ($R1 = 9.2\%$). For this reason a table of bond distances and angles is not included; we just note that the metal co-ordination geometries are unremarkable and entirely typical of other complexes containing {Mo($Tp^{Me,Me}$)(NO)Cl(py)} units.[19,20]

CCDC reference number 186/1715.

See http://www.rsc.org/suppdata/dt/1999/4341/ for crystallographic files in .cif format.

Acknowledgements

We thank the EPSRC (U.K.) for a Ph.D. studentship (to P. K. A. S.), and the European Commission for a TMR/Marie Curie fellowship (to A. B).

References

1 J. A. McCleverty and M. D. Ward, *Acc. Chem. Res.*, 1998, **31**, 842.
2 A. M. W. Cargill Thompson, D. Gatteschi, J. A. McCleverty, J. A. Navas, E. Rentschler and M. D. Ward, *Inorg. Chem.*, 1996, **35**, 2701.
3 V. Â. Ung, D. A. Bardwell, J. C. Jeffery, J. P. Maher, J. A. McCleverty, M. D. Ward and A. Williamson, *Inorg. Chem.*, 1996, **35**, 5290.
4 V. Â. Ung, A. M. W. Cargill Thompson, D. A. Bardwell, D. Gatteschi, J. C. Jeffery, J. A. McCleverty, F. Totti and M. D. Ward, *Inorg. Chem.*, 1997, **36**, 3447.
5 V. Â. Ung, S. M. Couchman, J. C. Jeffery, J. A. McCleverty, M. D. Ward, F. Totti and D. Gatteschi, *Inorg. Chem.*, 1999, **38**, 365.
6 D. C. Reitz and S. I. Weissman, *J. Chem. Phys.*, 1960, **33**, 700.
7 R. Brière, R.-M. Dupeyre, H. Lemaire, C. Morat, A. Rassat and P. Rey, *Bull. Soc. Chim. Fr.*, 1965, **11**, 3290.
8 B. Kirste, A. Kruger and H. Kurreck, *J. Am. Chem. Soc.*, 1982, **104**, 3850.
9 S. H. Glarum and J. H. Marshall, *J. Chem. Phys.*, 1967, **47**, 1374.
10 G. L. Closs and M. D. E. Forbes, *J. Am. Chem. Soc.*, 1987, **109**, 6185.
11 C. C. Parker, R. R. Reeder, L. B. Richards and P. H. Rieger, *J. Am. Chem. Soc.*, 1970, **92**, 5320.
12 A. Hasegawa, *J. Chem. Phys.*, 1971, **55**, 3101.
13 A. J. Amoroso, A. M. W. Cargill Thompson, J. P. Maher, J. A. McCleverty and M. D. Ward, *Inorg. Chem.*, 1995, **34**, 4828.
14 D. Collison, F. E. Mabbs and S. S. Turner, *J. Chem. Soc., Faraday Trans.*, 1993, 3705.
15 C. Elschenbroich, A. Bretschneider-Hurley, J. Hurley, A. Behrendt, W. Massa, S. Wocadlo and E. Reijerse, *Inorg. Chem.*, 1995, **34**, 743; C. Elschenbroich, A. Bretschneider-Hurley, J. Hurley, W. Massa, S. Wocadlo, J. Pebler and E. Reijerse, *Inorg. Chem.*, 1993, **32**, 5421; C. Elschenbroich, O. Schiemann, O. Burghaus and K. Harms, *J. Am. Chem. Soc.*, 1997, **119**, 7452; C. Elschenbroich, B. Metz, B. Neumüller and E. Reijerse, *Organometallics*, 1994, **13**, 5072.
16 R. Cook, J. P. Maher, J. A. McCleverty, M. D. Ward and A. Wlodarczyk, *Polyhedron*, 1993, **12**, 2111.
17 B. L. Westcott and J. H. Enemark, *Inorg. Chem.*, 1997, **36**, 5404.
18 J. A. Weil, J. R. Bolton and J. E. Wertz, *Electron Paramagnetic Resonance*, Wiley, New York, 1994.
19 S. L. W. McWhinnie, J. A. Thomas, T. A. Hamor, C. J. Jones, J. A. McCleverty, D. Collison, F. E. Mabbs, C. J. Harding, L. Yellowlees and M. G. Hutchings, *Inorg. Chem.*, 1996, **35**, 760.
20 R. Kowallick, A. N. Jones, Z. R. Reeves, J. C. Jeffery, J. A. McCleverty and M. D. Ward, *New J. Chem.*, 1999, **23**, 915.
21 H. M. Doesburg and J. H. Noordik, *Cryst. Struct. Commun.*, 1979, **8**, 377; G. P. M. van der Velden and J. H. Noordik, *J. Cryst. Mol. Struct.*, 1980, **10**, 83; G. M. Lobanova, *Kristallografiya*, 1968, **13**, 984.
22 M. More, G. Odou and J. Lefebvre, *Acta Crystallogr., Sect. B*, 1987, **43**, 398.
23 Molecular Mechanics program in the CAChe system, Oxford Molecular, Oxford, 1998.
24 J. P. Maher, J. A. McCleverty, M. D. Ward and R. D. Farley, unpublished results.
25 A. Hudson and G. R. Luckhurst, *Chem. Rev.*, 1969, **69**, 191.
26 P. K. A. Shonfield, Ph.D. Thesis, University of Bristol, 1999.
27 C. J. Jones, J. A. McCleverty, S. J. Reynolds and C. F. Smith, *Inorg. Synth.*, 1985, **23**, 4; S. Trofimenko, *Inorg. Chem.*, 1969, **8**, 2675; A. S. Drane and J. A. McCleverty, *Polyhedron*, 1983, **2**, 53.
28 W. E. Cleland, K. M. Barhhart, K. Yamanouchi, D. Collison, F. E. Mabbs, R. B. Ortega and J. H. Enemark, *Inorg. Chem.*, 1987, **26**, 1017.
29 G. M. Sheldrick, SHELXS 95 and SHELXL 95, University of Göttingen, 1995.
30 G. M. Sheldrick, SADABS, A program for absorption correction with the Siemens SMART area-detector system, University of Göttingen, 1996.

Paper 9/08138K